Harmonic Balance Vibration Analysis of Turbine Blades With Friction Dampers

Kenan Sanliturk, M. Imregun, David Ewins

Harmonic Balance Vibration Analysis of Turbine Blades With Friction Dampers

K. Y. Sanliturk, M. lmregun, D. J. Ewins

Imperial College of Science, Technology and Medicine Mechanical Engineering Department Exhibition Road, London SW7 2BX, UK

Although considerable effort has been devoted to the formulation of predictive models of friction damper behavior in turbomachinery applications, especially for turbine blades, the problem is far from being solved due to the complex nonlinear behavior of the contact surfaces. This paper primarily focuses on analytical and numerical aspects of the problem and addresses the problem in the frequency domain while exploring the viability of equivalent time-domain alternatives. The distinct features of this work are: (i) the modelling of nonlinear friction damper behavior as an equivalent amplitude-dependent complex stiffness via a first-order harmonic balance method (HBM), (ii) the use of sine sweep excitation in time-marching analysis, (iii) the application of the methodology to numerical test cases, including an idealised 3D turbine blade model with several friction dampers, (iv) the verification of the numerical findings using experimental data, and (v) a detailed assessment of the suitability of HBM for the analysis of structures with friction dampers.

1 Introduction

Friction dampers are widely used in turbomachinery applications in order to reduce resonant vibration amplitudes. Although considerable effort has been devoted to understanding and optimising friction dampers for such applications, the problem is far from being solved due to (i) lack of an appropriate mathematical description for contact interfaces, (ii) marked non-linearity of the contact dynamics, (iii) lack of reliable experimental data which can be used for empirical corrections, and (iv) the computational effort required to investigate large systems.

Several different models and associated solution strategies have been suggested in the past. The simplest interface representation is the well-known Coulomb friction model: contact points do not move with respect to each other unless the friction force exceeds a certain limit. Den Hartog (1931) was one of the first researchers to study the dynamic behavior of structures with Coulomb friction. The same interface model was applied to mistuned bladed-disk assemblies (Muszynska and Jones, 1983), to beams with various support conditions (Ferri and Bindemann, 1992), and to the stick-slip motion of turbine blade dampers (Pfeiffer and Hajek, 1992). Eventually, a series of damper stiffness was added to the basic Coulomb friction element to form the so-called ''macro-slip'' representation, and studies of turbine damper optimisation were conducted by Griffin (1980), Sinha and Griffin (1984), Menq and Griffin (1985), Chen and Sinha (1990) and Wang and Chen (1992).

The extensive use of the macro-slip model for friction interfaces is mainly due to its simplicity. However, over 30 years ago, it was already observed that friction interfaces could also exhibit micro-slip behavior characterized by partial slip at some parts of the interface before gross slip can occur (Goodman and Brown, 1962). Burtekin et al. (1978) represented the asperities by equal-stiffness prismatic rods, each behaving like a macro-slip element but the combined effect representing a micro-slip behaviour. Rogers and Boothroyd (1975) suggested an exponential curve to represent the observed load-displacement behavior of the friction interfaces. Later, Shoukry (1985) derived an analytical expression to relate the parameters of the exponential curve to the design parameters. Published work incorporating the micro-slip model in turbomachinery friction damping applications is relatively limited (Menq et al., 1986a, 1986b).

Most of the previous published work on turbomachinery blade friction damping is restricted to simple structural models with a small number of degrees-of-freedom. This is mainly due to the fact that the numerical solution is computationally very expensive due to the marked nonlinearity of the contact dynamics. Although a time-domain technique is, in principle, applicable to any number of degrees-of-freedom, practical limitations imposed by available computing power restrict its use in representative cases. Accordingly, current research is seeking efficient and accurate (albeit approximate) methods in the frequency domain, the harmonic balance method (HBM) being the most commonly used technique, a variant of which will also be employed here.

The main purpose of this paper is to focus on the analytical and numerical modelling issues of friction dampers in the frequency domain while exploring the viability of equivalent time-domain alternatives. The motivation behind this work is to develop a friction damper optimization technique which is capable of dealing with real geometries. The damper characteristics will be determined in a semi-empirical fashion by curve-fitting experimentally-acquired values, and the resulting nonlinear elements will be inserted into otherwise linear large-size FE models.

2 Harmonic Balance Formulation

2.1 Basic Theory. The harmonic balance method is frequently used for the dynamic analysis of nonlinear systems as an efficient alternative to expensive time-marching techniques (Menq and Griffin, 1985; Ferri and Bindemann, 1992; Wang and Chen, 1992). It is based on finding linearized coefficients which, in general, depend on both the frequency and the amplitude of the oscillation. In this particular study, the overall effect of the friction force will be expressed in terms of an amplitude-dependent complex stiffness representing the restoring and dissipative forces across a friction joint.

The HBM, which is also known as ''equivalent linearization method'' or ''describing function method,'' has its roots in electrical and control engineering (Gibson, 1963; Siljak, 1969). The most commonly used variant, the first-order HBM, is a fast

and accurate technique provided a number of conditions are satisfied (Mickens, 1984), the most serious limitation being that higher harmonic terms should have small amplitudes relative to the fundamental component. It is not intended here to give a detailed description of harmonic balance theory: a brief summary is provided for the sake of completeness. However, it should be noted that the present formulation is somewhat different from the usual approach: here the aim is to determine a linearized amplitude-dependent complex stiffness rather than simply calculating the first harmonic component of a nonlinear friction force, a route that has several advantages, as will be described in Section 3.

Now, let us consider the non-linear force-displacement relationship of a friction element given by:

$$F = F(x) \tag{1}$$

Assuming harmonic oscillation:

$$x = X \cos \omega t = X \cos \theta \tag{2}$$

The linearized stiffness coefficient, or the describing function of friction element, can be written as:

$$k^*_{eq}(X) = k^r_{eq}(X) + ik^i_{eq}(X) \tag{3}$$

where k^r_{eq} and k^i_{eq} are the amplitude-dependent real and imaginary parts of the equivalent stiffness, respectively. The first-order HBM adapted here is based on calculating the first harmonic component of the friction force in terms of the equivalent stiffness:

$$k^r_{eq}(X) = \frac{1}{\pi X} \int_0^{2\pi} F(X \cos \theta) \cos \theta d\theta \tag{4}$$

$$k^i_{eq}(X) = \frac{-1}{\pi X} \int_0^{2\pi} F(X \cos \theta) \sin \theta d\theta \tag{5}$$

2.2 Macro-slip Model and its Linearization. The macro-slip friction model of Fig. 1 has been used extensively in the analysis of various nonlinear systems and the linearized coefficients in terms of friction force are readily available in the literature (Wang and Chen, 1992). Accordingly, these force coefficients will be used here without any derivation but they will first be converted into equivalent complex stiffnesses because of the numerical advantages which will be discussed in Section 3.

Referring to Fig. 1, the real and imaginary parts of the amplitude-dependent equivalent stiffness are given by:

$$k^r_{eq} = \frac{K_d}{\pi} \left(\beta - \frac{1}{2} \sin (2\beta) \right) \tag{6}$$

$$k^i_{eq} = \frac{4N}{\pi X} \frac{X - X_{cr}}{X} \quad \text{for} \quad X \geq X_{cr} \tag{7}$$

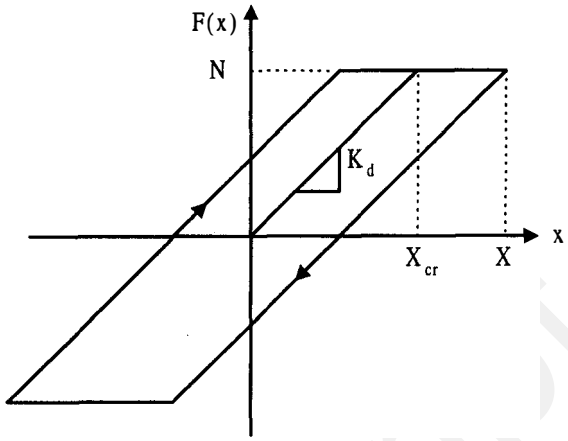

Fig. 1 Force-displacement relationship of macro-slip model

$$k^r_{eq} = K_d \tag{8}$$

$$k^i_{eq} = 0 \quad \text{for} \quad X < X_{cr} \tag{9}$$

where

$$X_{cr} = \frac{N}{K_d} \tag{10}$$

$$\beta = \cos^{-1} \left(\frac{X - 2X_{cr}}{X} \right) \tag{11}$$

2.3 Micro-slip Model and its Linearization. Although the macro-slip model above has the advantage of being simple, friction interfaces can also exhibit micro-slip behavior, i.e., partial slip at some parts of the contact surfaces before gross slip takes place. The main characteristic of micro-slip phenomena is that the slope of the loading curve (tangent stiffness) decreases gradually, due to partial slip, as the contact displacement increases (Rogers and Boothroyd, 1975; and Shoukry, 1985). The micro-slip model used here is also based on such an exponential loading curve which is shown in Fig. 2 and whose shape can be described by:

$$T(x) = ZK0(1 - e^{-\gamma x}) \tag{12}$$

where $ZK0$ and γ are the limiting friction force and hysteresis parameter of the micro-slip model, respectively.

The unloading (B to A) and reloading (A to B) curves for the steady-state condition are given by:

$$F_{BA}(x) = ZK0(1 - e^{-\gamma X}) - 2ZK0(1 - e^{-\gamma(X-x)/2}) \tag{13}$$

$$F_{AB}(x) = -ZK0(1 - e^{-\gamma X}) + 2ZK0(1 - e^{-\gamma(X+x)/2}) \tag{14}$$

Nomenclature

a = sweep rate
$[C]$ = viscous damping matrix
f = sinusoidal excitation force
F_o = amplitude of external sinusoidal excitation
F = friction force
$i = \sqrt{-1}$ or iteration number
k^r_{eq} = real part of linearized friction stiffness
k^i_{eq} = imaginary part of linearized friction stiffness
$[K]$ = stiffness matrix
K_d = friction stiffness at zero amplitude for macro-slip element
$[M]$ = mass matrix
N = limiting friction force for macro-slip element
r = mode number
t = time
T = loading curve for micro-slip model
θ = angular displacement
ω = angular velocity
x = response
X = amplitude of response level
X_{cr} = critical response level for macro-slip model (N/K_d)
$\{X\}$ = vector of response level amplitude
$ZK0$, γ = parameters of micro-slip model
η = modal damping

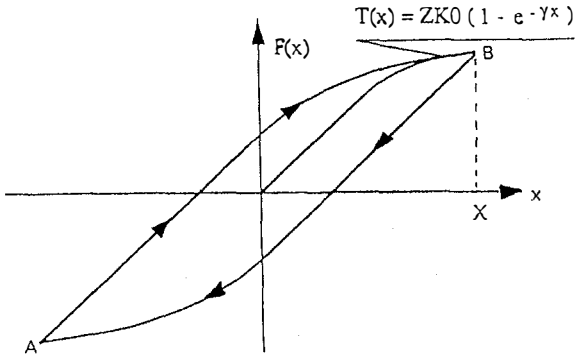

Fig. 2 Force-displacement relationship of micro-slip model

Assuming harmonic motion, Eqs. (13) and (14) can be written as

$$F_{BA}(X, \theta) = ZK0(1 - e^{-\gamma X}) - 2ZK0(1 - e^{-\gamma(X - X\cos\theta)/2}) \quad 0 < \theta \leq \pi \quad (15)$$

$$F_{AB}(X, \theta) = -ZK0(1 - e^{-\gamma X}) + 2ZK0(1 - e^{-\gamma(X + X\cos\theta)/2}) \quad \pi < \theta \leq 2\pi \quad (16)$$

Inserting Eqs. (15) and (16) into Eqs. (4) and (5) gives:

$$k^r_{eq}(X) = \frac{1}{\pi X}\left[\int_0^{\pi} F_{BA}(X, \theta)\cos\theta d\theta + \int_{\pi}^{2\pi} F_{AB}(X, \theta)\cos\theta d\theta\right] \quad (17)$$

$$k^i_{eq}(X) = \frac{-1}{\pi X}\left[\int_0^{\pi} F_{BA}(X, \theta)\sin\theta d\theta + \int_{\pi}^{2\pi} F_{AB}(X, \theta)\sin\theta d\theta\right] \quad (18)$$

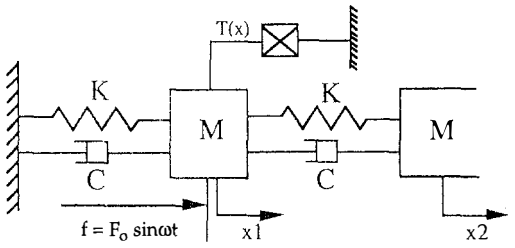

Fig. 4 A 2DOF system with friction element

Although the integrals in Eq. (18) are standard, those in (17) are not and hence the corresponding stiffness coefficient can only be obtained via numerical integration.

2.4 Linearized Stiffnesses for Macro- and Micro-slip Models. The complex equivalent friction stiffnesses for the macro- and micro-slip models were obtained as functions of the normalized displacement and the results are presented in Fig. 3. For the macro-slip model, the displacement axis is normalized with respect to the critical displacement X_{cr}, and the stiffness axis with respect to the linear friction stiffness K_d. In this format, the unit displacement represents the start of a slipping condition and the unit stiffness corresponds to the linear stiffness K_d.

For the micro-slip model, the stiffness axis is normalized with respect to the friction stiffness at zero displacement, and the displacement axis with respect to $1/\gamma$, this quantity representing an equivalent "critical displacement." As expected, the micro-slip model has an imaginary stiffness component for all displacement levels while the macro-slip model has an imaginary component if only the critical displacement has been exceeded.

3 Program Development

Two separate programs, one in the frequency domain and the other in the time domain, were developed to analyze structures with friction interfaces, the joint characteristics being described by a general loading curve including micro- and micro-slip elements.

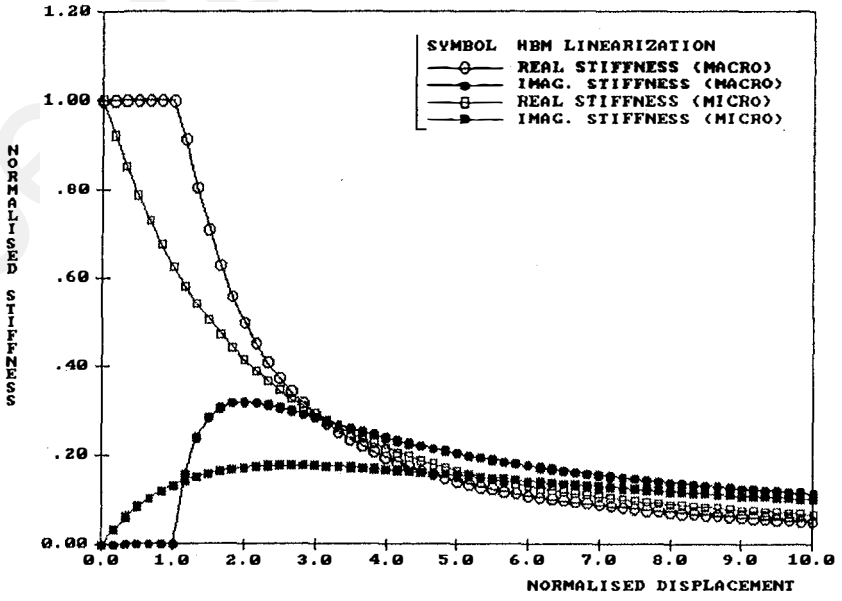

Fig. 3 Equivalent nonlinear friction stiffnesses for macro- and micro-slip elements

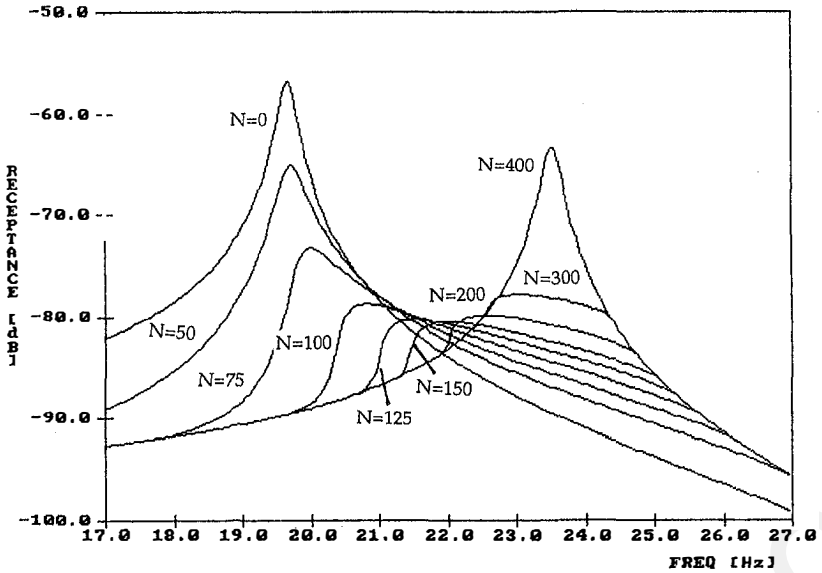

Fig. 5 FRFs for various friction limit case. (HBM analysis) (F_o = 100 N, K_d = 30000 N/m)

The solution algorithm adopted in the frequency-domain program is based on finding the response amplitudes iteratively, the starting point being the response levels of the underlying linear system. The relative displacement for each friction element is then computed and this value is used to determine a corresponding complex friction stiffness. The response amplitude is recomputed using this new stiffness value until convergence is achieved. The solution is considered to have converged if the ratio of the norm of the response increment vector to the norm of the response vector becomes less than a user-defined tolerance, i.e.,

$$\frac{\|\{X\}_i - \{X\}_{i-1}\|}{\|\{X\}_i\|} \leq Tol \qquad (19)$$

where i is the iteration number.

In the current implementation of the frequency-domain program, the frequency response function (FRF) matrix of the linear system is calculated at each frequency by forming the system matrix ($[K] - \omega^2[M] + i\omega[C]$) and solving a set of linear equations for the matrix inversion. The calculation of the non-linear response levels is performed iteratively via an efficient structural modification approach.

Expressing the friction force in terms of an equivalent complex stiffness has several advantages over using a linearised friction force directly. This approach is found to be especially appropriate for frequency-domain analyses since it allows the friction effects to be considered as external stiffness modifications. Also, the number of iterations at each frequency point can be reduced significantly by adopting this route. Furthermore, very efficient programs can be developed via sub-structuring or structural modification without having to factorise or invert the system matrix. These issues will be addressed in a forthcoming paper.

A time-domain vibration analysis program was developed in parallel to assess the advantages and shortcomings of the first-order accurate frequency-domain analysis. The implicit three-stage method by Thomas and Gladwell (1988), which is unconditionally stable when applied to linear systems, was used for

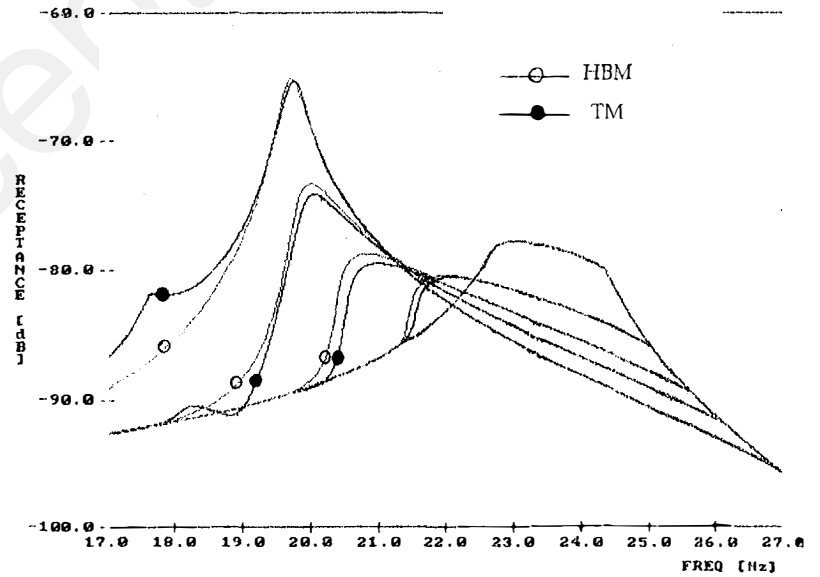

Fig. 6 Comparison of time-marching (TM) and HBM results (Limiting friction force from left to right = 50, 75, 100, 150, 300 N)

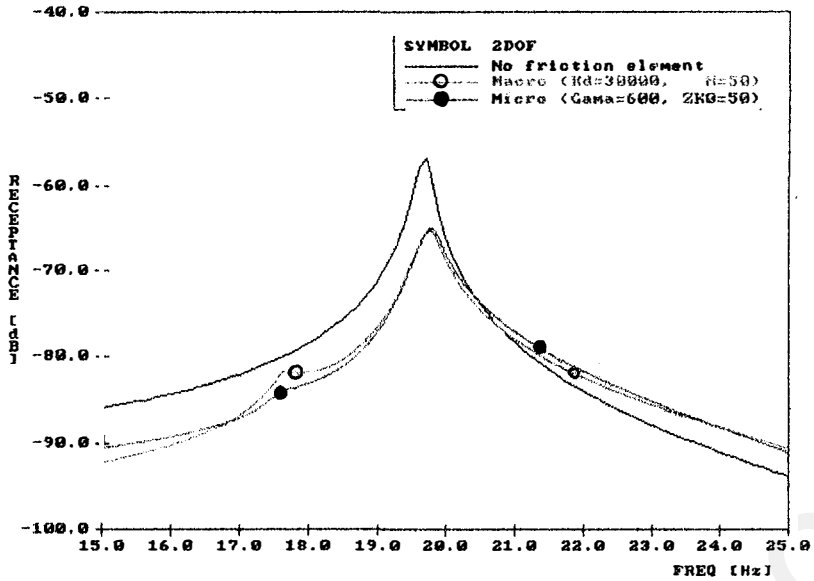

Fig. 7 Comparison of FRFs with 'equivalent' macro- and micro-slip models

the time-domain analysis. A variable time-step capability was also implemented in order to minimize the CPU time.

A continuous sine sweep excitation was used to cover the frequency range of interest. Although this type of excitation can reduce the CPU time significantly, one must choose the sweep rate carefully in order not to introduce significant natural frequency and damping errors due to transient effects. An approximate formula is given by Broch (1975) as:

$$a_r \leq (\eta_r \omega_r)^2 \tag{20}$$

where a_r is the sweep rate in Hz/sec, η_r and ω_r [Hz] being the modal damping and the natural frequency of the rth mode. If there are several modes within the frequency range of interest, the minimum sweep rate should be used. Furthermore, as the damping due to friction interfaces is not known prior to the analysis, existing linear damping need to be used in equation (20).

4 Case Studies

4.1 Case Study 1: 2 DOF Lumped Parameter Model. The 2DOF system, the simplest test case considered, is shown in Fig. 4 where the friction damper is indicated by a crossed-box. The model parameters of the system and the excitation amplitude are: M = 1.0 kg, K = 40.0 kN/m, C = 4.0 Ns/m and F_o = 100.0 N.

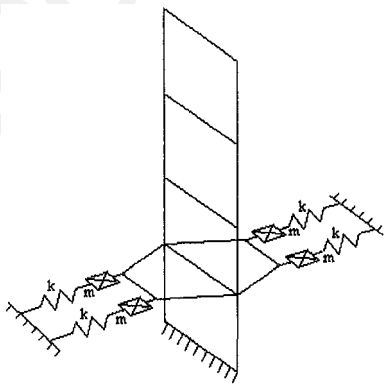

Fig. 8 Simplified 3D turbine blade model with friction dampers

Using a macro-slip element (K_d = 30 kN/m) and constant excitation load, the pseudo-receptance FRF, defined as the ratio of the nonlinear response to the excitation force both at co-ordinate 1, was obtained for various limiting friction force values between 0–400 N (Fig. 5). From a minimum response viewpoint, the optimum limiting friction force is observed to be 150 N.

The analysis was also carried out in the time domain and a comparison of the HBM and time-domain results are presented in Fig. 6 where the time-domain results indicate peak amplitudes rather than the amplitude of the response component at excitation frequency. The error introduced by using a first-order HBM seems to be small, with the response being overpredicted slightly around the resonances. However, the overall trend is captured very successfully and the optimum friction force value for the minimum response is determined with good accuracy. It should be noted that some of the time-marching curves show small peaks at around 18 Hz and these are due to the higher frequency content (three times the excitation frequency for this particular case) of the nonlinear friction force exciting the second mode of the system. As expected, a first-order HBM cannot predict such behavior since the higher terms are left out of the analysis.

The consequences of using macro- or micro-slip models to analyze friction damping were investigated next. The point receptance at co-ordinate 1 (''pseudo-receptance'' has been dropped for brevity) was calculated using ''equivalent'' macro- and micro-slip models for a limiting friction force of 50 N. The parameters of the macro- and micro-slip models were adjusted such that both models had the same friction stiffness at zero amplitude. Inspection of the results presented in Fig. 7 reveals that the responses are very close to each other with the exception of minor discrepancies. However, other results, not presented here, showed that this was not always the case, especially when the critical displacement limit is not reached. In such cases, the macro-slip model behaves linearly while the micro-slip model does not since it has no linear region.

4.2 Case Study 2: 3D MDOF Idealized Blade. The second test case was conducted using a 3D FE model of an idealised turbine blade with four identical macro-slip friction elements (Fig. 8). As it was desirable to check the results using a time-domain analysis, it was decided to use 32 co-ordinates only in order to save CPU time.

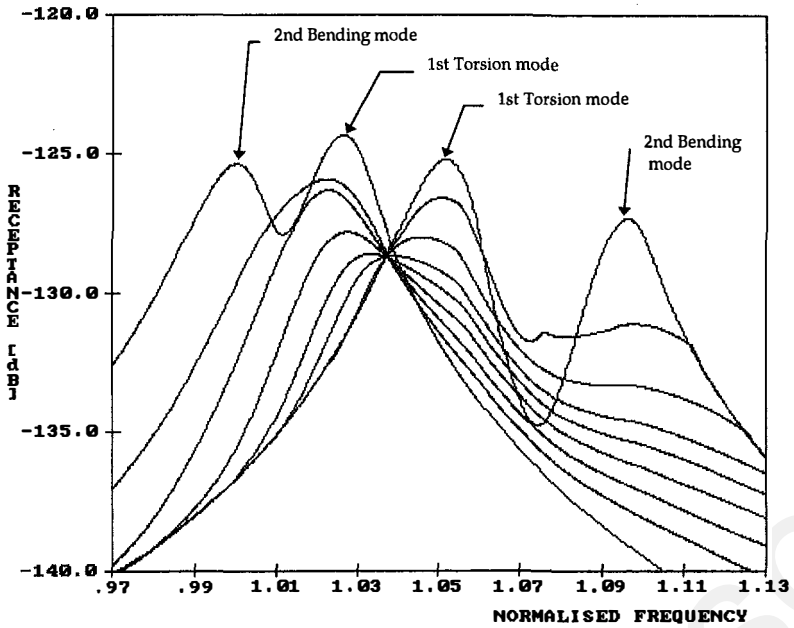

Fig. 9 Point FRFs from HBM analysis for various friction limit case (2nd bending and 1st torsion modes)

Response levels around the 2nd bending and the 1st torsion modes were computed for various limiting friction force values under constant excitation, the excitation point being the top corner of the blade in the flap bending direction. The results are plotted in Fig. 9. It is worthwhile to note that the bending and torsion modes switch over as the limiting friction force increases, a feature which must be considered duly when designing the friction dampers. The analysis was repeated using a time-domain method and very similar results were obtained. Both frequency- and time-domain results are presented in Fig. 10 for comparison purposes. It should be noted that the system is linear when the limiting friction force is zero ($N = 0$ N) or very large ($N = 10^5$ N), corresponding to free slipping and sticking conditions, respectively. Therefore, the HBM predictions are exact for these two limiting cases for which the first-order accuracy is not a restriction. A close inspection of Fig. 10 reveals that the time-domain results are shifted slightly towards the right hand side of the frequency axis but this discrepancy can be traced to the finite sine sweep rate used in the time-domain calculations. Bearing this effect in mind, one can say that the accuracy of HBM is excellent for this particular case study. However, it is difficult to generalise this result as the accuracy of a first-order implementation depends on both the strength of the nonlinearity and the location of the harmonics which, in turn, are related to the system's natural frequencies.

A comparison of the computational effort required by the time- and frequency-domain methods is presented in Table 1. It is immediately seen that the HBM requires about 1 percent of the CPU power needed by the time-marching analysis: a figure which is likely to decrease even further with the increasing number of co-ordinates. Therefore, the frequency-domain

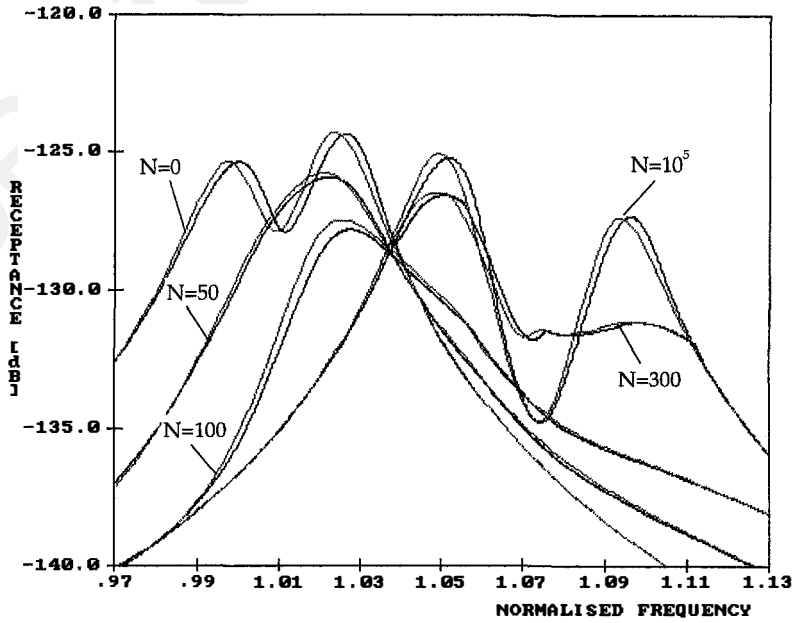

Fig. 10 Comparison of point FRFs from time-marching (TM) and HBM analyses (· · · ·: HBM, ——: TM)

Table 1 CPU times for frequency (HBM) and time (TM) domain analyses. Friction damper stiffness K_d = 50.0 MN/m, TM sine sweep rate = 2500 Hz/s; HBM at 200 frequency points

Friction parameters	CPU time		
Limiting friction force [N]	TM (seconds)	HBM (seconds)	HBM/TM (%)
50	9983	57	0.57
75	8440	63	0.75
100	7137	63	0.88
125	6752	65	0.96
150	6090	64	1.05
200	5247	47	0.90
300	4125	40	0.97

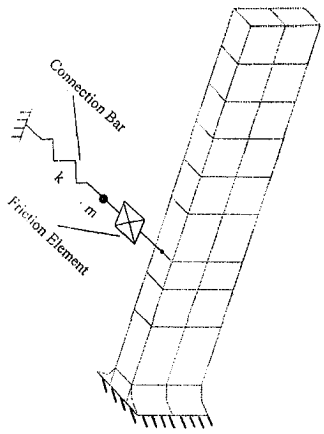

Fig. 11 Theoretical model of the test structure

technique seems to present a major advantage for analysing large-order nonlinear systems for friction damper optimization purposes.

4.3 Experimental Study: Correlation of Predicted and Measured Behavior. It was decided to conduct an experimental study with two specific objectives: (i) to validate the analytical predictions with experimental data, and (ii) to assess the applicability of the HBM technique to large models.

The test-rig comprised a cantilever beam, representing a simplified turbine blade and a friction damper attachment via a connection bar. The assembly was arranged such that the damper could be loaded by changing weights on a hanger. Additionally, a separate rig was designed to measure the friction joint characteristics. The friction damper was modelled as a hybrid element using a combination of macro- and micro-slip representations. The loading curve for the hybrid model was written, at a given displacement, as a linear combination of the loading curves of macro- and micro-slip models. The weighting factors for macro- and micro-slip models were functions of contact displacement. The parameters of this element—namely, the initial slope of the loading curve, the coefficient of friction and an empirical factor—were determined by a curve-fitting procedure using the measured data. Further details of the experimental set-up as well as the hybrid friction damper model can be found in Sanliturk et al. (1995).

A number of nonlinear response levels were measured for the 500–800 Hz frequency range, using normal loads of 0, 10, 12, 15, 20, 50, 100 and 200 N. The amplitude of the external force was kept constant at 10 N.

The idealized blade was modelled in 3D using finite elements and the final model including the connection bar and the friction damper (crossed-box) is shown in Fig. 11. The total number of degrees-of-freedom was 588, a size which would represent a formidable task for any nonlinear time-domain analysis.

Nonlinear response amplitudes were predicted using the frequency-domain program described in Section 3. The normal load values and the level of external excitation were kept the same as in the experiment, the frequency range being 500–800 Hz. A typical set of results is presented in Fig. 12 where the predicted and the measured nonlinear response levels for a constant excitation amplitude of 10 N are overlaid. It is immediately seen that the natural frequency of the mode at about 540 Hz (linear system) gradually increases to reach about 650 Hz, as the normal load increases (fully-stuck behaviour under a large friction force). It is also seen that there is an optimum normal load value (here about 20 N) for which the resonant response is at a minimum between the two limiting cases of 540 Hz and 650 Hz.

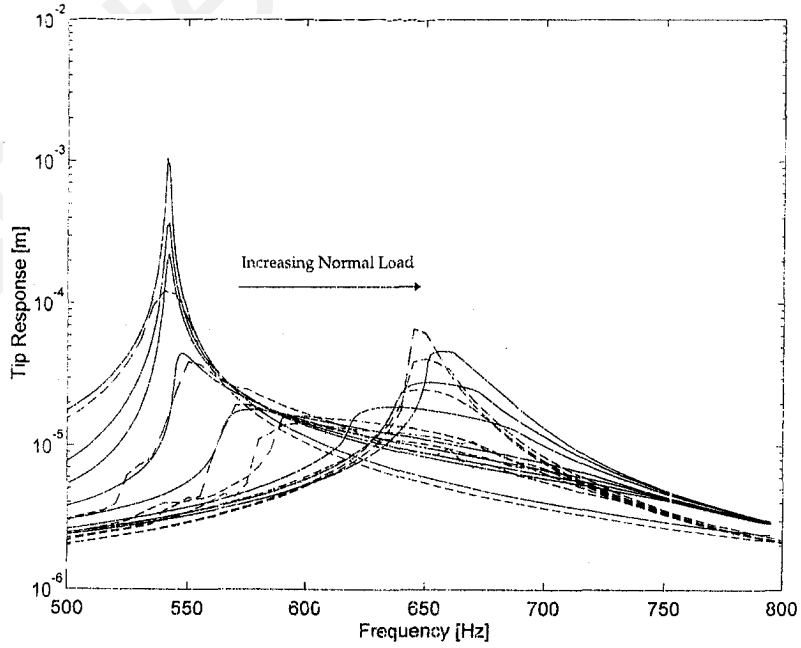

Fig. 12 Comparison of predicted and measured response levels (——: HBM predictions, – – –: Measured, Normal load = 0, 10, 12, 15, 20, 50, 100, 200 N)

In summary, the overall behavior, including the value of the optimum normal load, the resonant response levels and the natural frequency for the fully-stuck case, are all predicted with very good accuracy. A comparable nonlinear time-domain analysis could not be performed for this particular case as it proved to be computationally too expensive.

5 Concluding Remarks

(i) The frequency-domain formulation presented here is based on determining the linearized amplitude-dependent complex friction stiffness for both macro- and micro-slip elements. It has been found that dealing with a complex friction stiffness rather than the friction force directly is both easy to implement and reduces significantly the number of iterations required for convergence.

(ii) Both macro- and micro-slip friction models may give similar results for predicting the response levels of systems with friction dampers, provided that the response level exceeds the critical displacement for the macro-slip friction model.

(iii) Applying a continuous sine sweep excitation can reduce substantially the CPU time required in a time-marching analysis without introducing significant natural frequency and damping errors, provided the sweep rate is chosen properly. However, time-marching analysis is still very expensive compared with HBM, especially when analyzing large-order nonlinear systems.

(iv) The numerical findings of the frequency-domain technique have been validated against experimental data and the agreement between the predicted and measured response data was found to be very good.

(v) Analyzing bladed-disk systems with friction dampers using the HBM is very efficient and qualitative predictions seem to be acceptable. Therefore, the use of the HBM is recommended in order to optimize friction dampers in turbomachinery applications. In any case, no viable alternatives seem to exist when full-size finite element models need to be employed.

6 Acknowledgments

The authors are grateful to their sponsors, Rolls-Royce plc, for their permission to publish this work. The authors also thank R. Tuley and J. Green of Rolls-Royce for conducting some of the time-marching calculations. They also acknowledge the contribution of A. B. Stanbridge for acquiring the experimental data.

7 References

Broch, T. J., 1975, *On the Measurement of Frequency Response Functions,* B&K Tech. Rev. No. 4.

Burtekin, M., Cowley, A., and Back, N., 1978, "An Elastic Mechanism for the Micro-sliding Characteristics Between Contacting Machined Surfaces," *Journal of Mechanical Engineering Science,* Vol. 20, No. 3, pp. 121–127.

Chen, S., and Sinha, A., 1990, "Probabilistic Method to Compute the Optimal Slip Load for a Mistuned Bladed Disc Assembly With Friction Dampers," ASME JOURNAL OF VIBRATION AND ACOUSTICS, Vol. 112, pp. 214–221.

Den Hartog, J. P., 1931, "Forced Vibrations with Combined Coulomb and Viscous Friction," *Transactions of ASME,* Vol. 53, pp. 107–115.

Ferri, A. A., and Bindemann, A. C., 1992, "Damping and Vibration of Beams With Various Types of Frictional Support Conditions," ASME JOURNAL OF VIBRATION AND ACOUSTICS, Vol. 114, pp. 289–296.

Gibson, J. E., 1963, *Non-linear Automatic Control,* McGraw-Hill Book Comp.

Goodman, L. E., and Brown, C. B., 1962, "Energy Dissipation in Contact Friction: Constant Normal and Cyclic Tangential Loading," ASME *Journal of Applied Mechanics,* pp. 17–22, March.

Griffin, J. H., 1980, "Friction Damping of Resonant Stresses in Gas Turbines Airfoils," ASME *Journal of Engineering for Power,* Vol. 102. No. 2, pp. 329–333.

Menq, C-H., Bielak, J., and Griffin, J. H., 1986a, "The Influence of Microslip on Vibratory Response, Part II: Comparison with Experimental Results," *Journal of Sound and Vibration,* 107 (2), pp. 295–307.

Menq, C-H., Griffin, J. H., and Bielak, J., 1986b, "The Forced Vibration of Shrouded Fan Stages," ASME JOURNAL OF VIBRATION ACOUSTICS, STRESS AND RELIABILITY IN DESIGN, Vol. 108, pp. 50–55.

Menq, C-H., and Griffin, J. H., 1985, "A Comparison of Transient and Steady State Finite Element Analyses of the Forced Response of a Frictional Damped Beam," ASME JOURNAL OF VIBRATION ACOUSTICS, STRESS AND RELIABILTY IN DESIGN, Vol. 107, pp. 19–25.

Mickens, R. E., 1984, "Comments on the Method of Harmonic Balance," *Journal of Sound and Vibration,* Vol. 94, No. 3, pp. 456–460.

Muszynska, A., and Jones, D. I. G., 1983, "On Tuned Bladed Disk Dynamics: Some Aspects of Friction Related Mistuning," *Journal of Sound and Vibration,* Vol. 86, No. 1, pp. 107–128.

Pfeiffer, F., and Hajek, M., 1992, "Stick-Slip Motion of Turbine Blade Dampers," *Philosophical Transactions of the Royal Society of London,* Series A, Vol. 338, No. 1651, pp. 503–517.

Rogers, P. F., and Boothroyd, G., 1975, "Damping at Metallic Interfaces Subjected to Oscillating Tangential Loads," ASME *Journal of Engineering for Industry,* pp. 1087–1093.

Sanliturk, K. Y., Stanbridge, A. B., and Ewins, D. J., 1995, "Friction Dampers: Measurement, Modelling and Application to Blade Vibration Control," ASME 15th Biennial Conference on Vibration and Noise, Boston USA, 17–21, September, DE-Vol. 84-2, pp. 1377–1382.

Shoukry, S. N., 1985, "A Mathematical Model for the Stiffness of Fixed Joints Between Machine Parts," *Proc. Int. NUMETA Conf.,* Swansea, U.K., pp. 851–858.

Siljak, D., 1969, *Non-linear Systems: A Parameter Analysis and Design,* John Wiley and Sons.

Sinha, A., and Griffin, J. H., 1984, "Effects of Static Friction on the Forced Response of Frictionally Damped Turbine Blades," ASME *Journal of Engineering for Gas Turbines and Power,* Vol. 106, pp. 65–69.

Thomas, R. M., and Gladwell, I., 1988, "Variable-Order, Variable-Step Algorithms for Second-Order Systems. Part 1: The Methods, Part 2: The Codes," *International Journal for Numerical Methods in Engineering,* Vol. 26, pp. 55–80.

Wang, J. H., and Chen, W. K., 1992, "Investigation of the Vibration of a Blade with Friction Damper by HBM," ASME, 92-GT-8, Presented at the International Gas Turbine and Aeroengine Congress and Exposition, Cologne, Germany, June 1–4.